



# NUMERICAL INVESTIGATION OF THERMOMECHANICAL BEHAVIOUR AND MICROSTRUCTURE EVOLUTION OF A NICKEL ALLOY WORKPIECE DURING ITS UPSETTING

A.A. Rogovoy and N.K. Salikhova

*Institute of Continuous Media Mechanics UB RAS, Perm, Russian Federation*

The use of science-based technologies in commercial production makes it possible to obtain high-quality, competitive finished products. The development of new techniques or optimization of existing technological processes involving the in-depth experimental research is resource-intensive and time-consuming. In this regard, numerical simulation of the technological process under study can be used as an alternative to a physical experiment. The results obtained by numerical methods will make it possible to substantiate the most appropriate regime of billet deformation, providing the required changes in the structure of the material. This paper considers a specific technological process of hot forming by pressure of a massive billet, which includes two stages: air cooling of the billet while transporting it from the furnace to deforming tools and forming operation – free upsetting of a billet with the aid of a moving upper flat plate and a stationary cutting lower plate. Computer simulation of upsetting of a large billet with the aim to define a change in its shape, temperature distribution over the surface and throughout the billet, and deformation inhomogeneity arising in the process of hot forming was carried out using the Deform-2D/3D software package. The initial temperature distribution of material during pressure forming is determined by modeling air cooling of the billet for 45 seconds during its transportation from the furnace to the deforming equipment. For the obtained inhomogeneous temperature distribution, the calculations were performed to evaluate the force required for billet upsetting to the technology specified average diameter of about 1060 mm at a die movement of 100 mm/s. The Johnson–Mehl–Avrami–Kolmogorov (JMAK) model was used to investigate the evolution of the microstructure (average grain size and recrystallized volume fraction) of the Waspalloy nickel alloy generated as a result of dynamic recrystallization during hot forming of a billet at a strain rate of 100 mm/s.

**Key words:** hot forming, heat-resistant nickel alloy Waspalloy, dynamic recrystallization, finite element method, Johnson–Mehl–Avrami–Kolmogorov model

## 1. Introduction

Heat-resistant alloys of the "Ni-Cr-Fe" system, developed in the late 1930s, are successfully used in the aerospace industry. Such alloys can operate for a long time under intensive static and dynamic loads at high temperatures and maintain stable mechanical properties. For example, the operating temperature of modern nickel-based heat-resistant alloys reaches  $\sim 1100^{\circ}\text{C}$ . One of the most commonly used commercial nickel alloys is Waspalloy, which has found wide application in the production of some elements of aircraft gas turbine engines (rotating and nozzle blades, turbine rotor disks, etc.) with a maximum operating temperature of  $\sim 870^{\circ}\text{C}$ .

This paper contains the results of the continuation of our previous study [1], where the effect of the strain rate on the evolution of microstructure during hot plastic forming of a billet of the Waspalloy nickel alloy is considered. The material microstructure was characterized by the average grain size and the volume fraction of the recrystallized part of grains. The influence of the process parameters on the formation of the Waspalloy alloy structure was estimated based on the results of calculation of thermal and strain states of a massive billet during its free upsetting at the speed of upper flat die of 50 and 100 mm/s. The change in the microstructure (the formation of low-defect "nuclei" of new grains and their subsequent growth), which occurs as a result of plastic deformation, is known as a process of dynamic recrystallization [2]. To describe the kinetics of this process, the Johnson-Mel-Avrami-Kolmogorov model was used in [1]. It was found that the structure formed at a speed of the upper die of 100 mm/sec has finer grain size than the structure formed at a speed of 50 mm/sec. In the first case, the average grain size in the area of the most intensive deformation was  $13,9\ \mu\text{m}$ , whereas in the second case it was  $14,4\ \mu\text{m}$ , with an average initial grain size of  $\sim 25\ \mu\text{m}$ . It was also shown that at higher upsetting rate (100 mm/s) the process of dynamic recrystallization proceeds more intensively and involves a larger volume of material.

In a real technological process, the billet is first heated in a furnace to the temperature that provides the best plasticity during plastic working and then transferred to the deforming equipment, in which it is upset to

a diameter defined by the technology standards. During its transporting, the billet cools down, which leads to a non-uniform temperature distribution. The latter, being initial for the subsequent upsetting process, affects the dynamic recrystallization, which significantly depends on the strain level and temperature. Therefore, it makes sense to analyze the microstructure evolution taking into account air the cooling of a massive billet during its transportation to the deforming equipment.

The present work investigates the influence of the initial temperature distribution, formed as a result of billet cooling in air as it is transported from the furnace to the deforming equipment, on the changes occurring in the microstructure of the Waspaloy alloy. On the basis of our earlier studies, described in [1], the speed of movement of the upper striking plate is taken equal to 100 mm/s.

It is known that the mechanical properties of metals and alloys (such as strength, plasticity, impact toughness and others) depend on the structure of polycrystalline billet [2–4]. The most important structural parameter is the grain size. The process of hot forming causes the grain size reduction (grain refinement), which increases the strength and plastic properties of metals [5]. This process includes forging, stamping, pressing, drawing, and others [6, 7]. Upsetting of shank-ended billet is the main operation in free forging, which is carried out before the drawing (pressing) process to improve the quality and structure of the metal. It is this operation that is the focus of the present study. Subsequent drawing of the billet is not considered here.

The technological process of hot forming of a large billet to obtain the specified geometric dimensions under a certain temperature-dynamic pressure action includes the stage of its cooling in the air for 45 seconds, while transporting it from the furnace to the deforming equipment and the stage of free upsetting. The purpose of modeling is to study changes that occur in the material microstructure during hot plastic deformation. As in [1], the Waspaloy metal alloy was chosen as a test material for studying the evolution of grain structure; its microstructure is described using a set of parameters.

Computer simulation was carried out using the Deform-2D/3D software package [8, 9]. It is based on the finite element method and makes it possible to analyze the change in the billet shape occurred during different forming operations and evaluate the stress-strain and thermal state throughout the billet during hot forging, taking into account geometric and physical nonlinearities.

The object of the study is a massive billet weighing 9300 kg, which is shown in Figure 1. The billet consists of a body and a shank (pivot). In the initial state, the body of the billet has the form of a truncated octahedral pyramid with the area of the lower base of  $\sim 6050,18 \text{ cm}^2$  and the upper base  $\sim 4812,75 \text{ cm}^2$ . The shank is a cylinder 500 mm high and 300 mm in diameter.

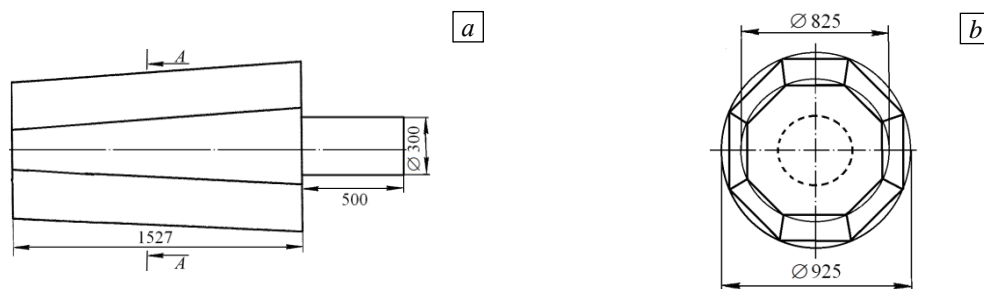


**Fig. 1.** Billet with initial geometric dimensions, mm: front view (a), left view (b); cross section A-A passes through the middle of the billet body and is perpendicular to its central axis.

A three-dimensional model of the billet constructed with the aid of SolidWorks program is shown in Figure 2a. An example of tetrahedral discretization, in which the computational domain is decomposed into a certain number of tetrahedral finite elements, is shown in Figure 2b. The discrete analogue of the examined three-dimensional body contains 52168 finite elements (the optimal number of elements determined by numerical experiments) and 11298 nodal unknowns. The mesh is constructed with account of complexity of the object geometry, so that the mesh density is increased at its boundaries. During plastic working, only the body of the billet is subjected to deformation, while the shape of the shank, which serves to hold the billet in the process of upsetting, remains unchanged. However, the shank cannot be disregarded in modeling because it affects the rate of cooling of the bottom surface of the billet. As a result, the finiteelement mesh in this area becomes less dense.

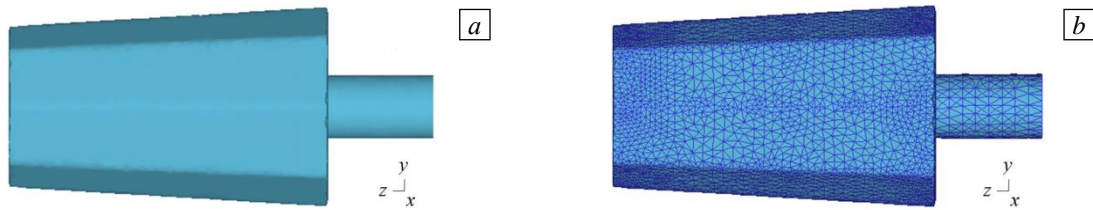


**Fig. 2.** Volumetric model of the billet (a), built with the aid of the SolidWorks software, and its finite-element discretization (b).

## 2. Air cooling of the billet during transportation to the deforming equipment

A massive billet is subjected to pressure forming according to the following technological scheme. Before the beginning of deformation — the process of free upsetting — the billet is heated and kept in the fuel-fired furnace until it reaches a temperature of 1000°C uniformly distributed throughout the billet. The heating process itself is not included in the modeling process. The billet is then transported by air from the furnace to the deforming equipment for 45 s, which leads to its cooling. The resulting temperature distribution is assumed to be reference for further free upsetting operation.

The equation of nonstationary heat conduction, which allows us to calculate the temperature field inside the billet and on its surface, is written as [10, 11]:

$$\rho c \frac{\partial T}{\partial t} = \nabla \cdot (k \nabla T) + Q. \tag{1}$$

Here:  $\rho$  is the material density in the current state, kg/m<sup>3</sup>;  $c$  is the specific heat capacity, J/(kg·K);  $T$  is temperature on the absolute scale, K;  $\nabla$  is Hamilton's operator for the current configuration;  $k$  is heat conductivity coefficient, W/(m·K);  $Q$  is the power of internal sources of heat generation (heat absorption), W/m<sup>3</sup>;  $t$  is the current time, s.

For the equation of nonstationary thermal conductivity (1) it is necessary to set the initial condition in the form of temperature distribution inside the body and on its surface  $S$  at the initial moment of time, as well as the boundary conditions. Thus, on the surface  $S = S_T \cup S_q$  they are as follows:

$$\begin{array}{ll} \text{on the part } S_T & T = T^*, & 1 \\ \text{on the part } S_q & -\mathbf{N} \cdot k \nabla T = q_N, & 2 \end{array} \tag{2}$$

where  $T^*$  is the prescribed value of absolute temperature,  $\mathbf{N}$  is the external unit normal to the body surface in the current state,  $q_N = \alpha_\Sigma (T - T_c)$  is the component of heat flow through the boundary normal to the body surface, where  $T_c$  is ambient temperature on the absolute scale,  $\alpha_\Sigma$  is the heat transfer coefficient, which is calculated as

$$\alpha_\Sigma = \alpha_s + \alpha_r.$$

In the last expression  $\alpha_s$  is the coefficient of heat transfer by convection, W/(m<sup>2</sup>·K), and  $\alpha_r$  is the coefficient of heat transfer by radiation, which is calculated by the formula

$$\alpha_r = \frac{\sigma_0 \varepsilon_m^{eff} (T^4 - T_c^4)}{T - T_c},$$

where  $\sigma_0 = 5,67 \cdot 10^{-8}$  W/(m<sup>2</sup>·K<sup>4</sup>) is the Stefan-Boltzmann constant,  $\varepsilon_m^{eff}$  is the effective degree of blackness of the material (for the Waspaloy alloy this value in the database of the Deform-2D/3D package is 0,7).

As the boundary conditions on the lateral and end surfaces of the examined body we set the conditions for radiation and convective heat transfer in a simplified form, i.e. they are reduced to convective heat transfer. The contribution of radiant heat transfer is taken into account according to the above formula for the radiation heat transfer coefficient. During transportation of the massive billet from the furnace to the forging

tools, where the process of free upsetting takes place, ambient temperature is assumed to be 20°C. In this case, the convective heat transfer coefficient is 20 W/(m<sup>2</sup>·K) [14].

A constant temperature distribution in the billet equal to 1000°C is taken as the initial condition. In this study we used the scales of Kelvin and Celsius. The relationship between the scales is determined by a well-known formula, in which the absolute temperature is obtained by adding the value of 273,15 to the temperature in degrees Centigrade.

The temperature-dependent thermophysical properties of the Waspaloy nickel alloy are taken from the library of the Deform-2D/3D software. The curves of the coefficient of thermal conductivity and specific heat capacity are shown in Figure 3.

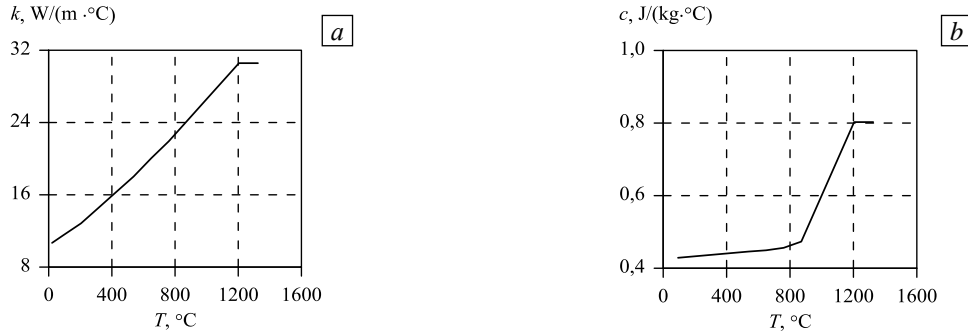


**Fig. 3.** Temperature dependences of thermal conductivity coefficients (a) and specific heat capacity (b).

The heat conduction equation (1) and boundary conditions (2) correspond to the variation equation:

$$\int_V [(c\rho\dot{T} - Q)\delta T + k\nabla T \cdot \nabla(\delta T)]dV + \int_{S_q} q_N \delta T dS = 0. \tag{3}$$

It is obtained by applying the Galerkin procedure to equation (1) and boundary condition (2)<sub>2</sub>, which are represented in the homogeneous form with account of the fact that the regions  $V$  and  $S_q$  do not intersect:

$$\int_V [c\rho\dot{T} - \nabla \cdot (k\nabla T) - Q]\delta T dV + \int_{S_q} (\mathbf{N} \cdot k\nabla T + q_N)\delta T dS = 0. \tag{4}$$

If we choose the function  $T$ , which satisfies boundary condition (2)<sub>1</sub> on the part of the surface  $S_T$ , i.e.  $T = T^*$ , then on the part  $S_T$ , the variation is  $\delta T = 0$ . Then the second integral in (4) can be calculated not over the part  $S_q$ , but over the entire surface that bounds the volume  $V$ . In this case, the Ostrograd–Hauss theorem applies to the first term of the second integral:

$$\int_S \mathbf{N} \cdot k\nabla T \delta T dS = \int_V \nabla \cdot (k\nabla T \delta T) dV.$$

Then, using the relation  $\nabla \cdot (\alpha\mathbf{b}) = (\nabla\alpha) \cdot \mathbf{b} + \alpha(\nabla \cdot \mathbf{b})$ , where  $\alpha$  is any scalar,  $\mathbf{b}$  is any vector, we can easily represent the integral in the right-hand side in the following form (assuming that  $\alpha = \delta T$ ,  $\mathbf{b} = k\nabla T$ ):

$$\int_V \nabla \cdot (k\nabla T \delta T) dV = \int_V \delta T [\nabla \cdot (k\nabla T)] dV + \int_V k\nabla T \cdot \nabla(\delta T) dV,$$

which is just the representation that yields variational equation (3). In this equation, the volume and surface refer to the current state and are undefined quantities until the problem is solved. But they can be easily reduced to the known volume and surface of the body in the initial state. Taking into account the fact that the elementary mass does not change:  $dm = \rho dV = \rho_0 dV_0$ , where  $\rho_0$ ,  $dV_0$  are the density of material and the elementary volume in the initial state, as well as the expression relating the elementary volumes in the current and initial configurations  $dV = JdV_0$  to the elementary surfaces in these configurations

$dS = J\sqrt{\mathbf{n} \cdot \mathbf{C}^{-1} \cdot \mathbf{n}} dS_0$  where  $J$  is the third invariant of the space gradient  $\mathbf{F}$ ,  $\mathbf{C} = \mathbf{F}^T \cdot \mathbf{F}$  is the Cauchy-Green deformation measure,  $\mathbf{n}$  is the outward normal to the surface in the initial configuration, we can reduce the variational equation (3) to the following constructive form:

$$\int_{V_0} [(c\rho_0 \dot{T} - JQ)\delta T + Jk\nabla T \cdot \nabla(\delta T)] dV_0 + \int_{S_q^0} J\sqrt{\mathbf{n} \cdot \mathbf{C}^{-1} \cdot \mathbf{n}} q_N \delta T dS_q^0 = 0. \tag{5}$$

The Hamiltonian operator of the current state  $\nabla$  entering into this expression can be transformed to the Hamiltonian operator of the initial state  $\overset{0}{\nabla}$ , by making use of the relationship:  $\nabla = \mathbf{F}^{-T} \cdot \overset{0}{\nabla}$ . In the Deform 2D/3D software package equation (5) is implemented by the finite element method.

Air cooling of a large billet during its transportation to the deforming equipment is not accompanied by any inner heat generation or heat sink, so that in (5)  $Q=0$ . In this process, the current configuration coincides with the initial configuration, from which it follows that  $J=1$ ,  $\mathbf{F} = \mathbf{C} = \mathbf{g}$ , ( $\mathbf{g}$  is a unit tensor), which significantly simplifies equation (5). The results obtained with this equation are given in Figure 4 to illustrate changes in temperature of the billet after its cooling in the air.

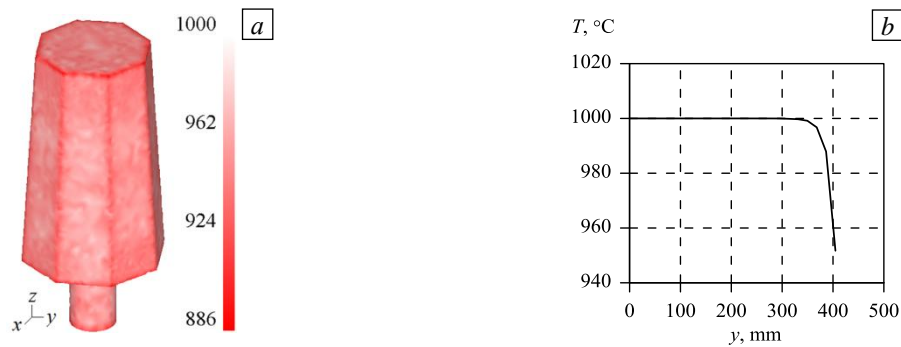


**Fig. 4.** Temperature distribution over the billet surface after its cooling in the air for 45 s during its transportation to the equipment (a); graph of temperature variation with a distance to the center of the billet in section A–A (see Fig. 1b).

The temperature of the lateral surface of the massive billet changes by about 47°C in the "narrow" near-surface region (see Fig. 4b). A decrease in the billet temperature is observed at a distance of ~91 mm from the surface, however at greater depth the billet temperature does not change. Besides, there are areas in the billet body where temperature has minimum value of ~915°C. These areas are located on the ribs of the billet and in the lower part of the shank. The average temperature values at the upper and lower ends of the billet and at the surface of the shank are approximately ~943–958°C. In the following, the calculated temperature distribution is used as the reference one in the analysis of the strain state arising in the billet during its upsetting at the second stage of the technological process.

### 3. Free upsetting of a massive shank–ended billet

Then, according to the hot forming technology, the billet is upset by plane-parallel plates - movable upper plate and fixed lower plate with a hole for the shank with diameter of 300 mm. The upper plate, which moves downwards along the vertical axis  $z$  with a speed of 100 mm/s to the distance  $u_z = 496$  mm, deforms the billet. To prevent significant cooling of the billet as it comes in contact with the deforming plates, they are heated to a temperature of 400°C. Since in a real technological process, the strikers are deformed insignificantly, in the model, they are assumed to be absolutely rigid. The friction arising between the striking plates and the billet during hot forming is described using Siebel's law, in which the friction force is defined as the product of the friction coefficient by the value of tangential stress. Since the nickel-based heat-resistant Waspaloy alloy is a hard-to-treat material, its deformation proceeds with the application of a lubricant, which reduces the effect of friction forces on the contact surface and reduces the deformation force. The friction coefficient  $\mu$  is taken constant and equal to 0,3. With such coefficient of friction, the average diameter of the billet, according to technological requirements, should be ~1060 mm, which is achieved at an average axial degree of deformation of ~32,5%. The value of the latter is calculated by the formula:

$$\varepsilon_h = (l_0 - l_1) \cdot 100\% / l_0 = \Delta l \cdot 100\% / l_0,$$

where  $l_0$  is the initial height of the billet;  $l_1$  is the height of the billet after completion of the upsetting process,  $\Delta l = l_0 - l_1$  is the amount of upsetting.

Free upsetting of the billet is a slow- running process, so that in the numerical simulation the inertial forces acting on the billet are not taken into account. In the practice of theoretical calculations for metal forming, in most cases only plastic strains are considered; assumptions are made about the inessential influence of mass forces on the alloy flow [15], and elastic strains are negligible. In this case, the mathematical formulation of the problem of determining the stress–strain state of the billet in the process of hot forming includes the following equations [1, 12, 13]:

- equation of equilibrium  $\nabla \cdot \mathbf{T} = 0$ ;
- kinematic equation for the velocity deformation  $\dot{\boldsymbol{\varepsilon}} = [\nabla \mathbf{v} + (\nabla \mathbf{v})^T] / 2$ ;
- incompressibility equation  $I_1(\dot{\boldsymbol{\varepsilon}}) = \nabla \cdot \mathbf{v} = 0$ ;
- Levy–Mises plastic flow equation  $\dot{\boldsymbol{\varepsilon}} = 3 \dot{\bar{\varepsilon}} \mathbf{S} / (2 \bar{\sigma})$ ;
- Mises plasticity condition  $\bar{\sigma} = \sigma_s$ .

In the above equations, the following notation is used:  $\nabla$  is the Hamilton operator in the current configuration;  $\mathbf{T}$  is the Cauchy stress tensor (true stresses);  $\dot{\boldsymbol{\varepsilon}}$  is the velocity deformation tensor;  $\mathbf{v}$  is the displacement velocity vector of an arbitrary billet point;  $I_1(\dot{\boldsymbol{\varepsilon}})$  is the first invariant of the tensor  $\dot{\boldsymbol{\varepsilon}}$ ;  $\mathbf{S}$  is the stress tensor deviator;  $\sigma_s$  — is the flow stress of material;  $\bar{\sigma}$  is the effective stress ( $\bar{\sigma} = \sqrt{(3/2) \mathbf{S} \cdot \mathbf{S}}$ );  $\dot{\bar{\varepsilon}}$  is the effective strain rate ( $\dot{\bar{\varepsilon}} = \sqrt{(2/3) \dot{\boldsymbol{\varepsilon}} \cdot \dot{\boldsymbol{\varepsilon}}}$ ).

The flow stress of material ( $\sigma_s$ ) is the function of the accumulated effective strain ( $\bar{\varepsilon}$ ), effective strain rate ( $\dot{\bar{\varepsilon}}$ ) and absolute temperature ( $T$ )

$$\sigma_s = \sigma_s(\bar{\varepsilon}, \dot{\bar{\varepsilon}}, T), \quad \bar{\varepsilon} = \int \dot{\bar{\varepsilon}} dt.$$

For the Waspaloy alloy, the flow stress is given in a tabulated form for the temperature range 954,5–1148,9 K the range of effective strain rate 0,032–1,000  $\text{c}^{-1}$  and the range of effective strain 0–0,9. As stated in work [1], it is just these ranges of the above quantities, in which the examined technological process takes place. During deformation the quantities  $T$ ,  $\bar{\varepsilon}$ ,  $\dot{\bar{\varepsilon}}$  vary from point to point. Therefore, depending on their values, the flow stress  $\sigma_s$  will also differ from point to point. For example, at 1000°C,  $\bar{\varepsilon} = 0,35$ ,  $\dot{\bar{\varepsilon}} = 0,032$ , the flow stress  $\sigma_s$  is approximately 339,62 MPa. Here, it is to be noted that the table, presenting data from the Deform-2D/3D software library, does not contain the value of the flow stress for the temperature of 1000°C. The corresponding value was found by the linear interpolation. Interpolation and extrapolation will be used further when working with this table.

To close the formulation of the boundary value problem, the equations written above are supplemented with the following boundary conditions: on the part  $S_v$  of the surface  $S$ , that bounds the current volume of the deformed body  $V$ , we specify the displacement velocity as  $\mathbf{v} = \mathbf{v}^*$ , and on the part  $S_p$  — the external forces:  $\mathbf{p}^* = \mathbf{N} \cdot \mathbf{T}$ . Here  $S = S_v \cup S_p$  is the entire instantaneous surface of the body.

Applying the standard Galerkin procedure to the equations of equilibrium, incompressibility and boundary conditions for stresses presented in a homogeneous form, and taking into account the fact that the regions  $V$  and  $S_p$  do not intersect and the variations  $\delta \mathbf{v}$  and  $\delta \sigma$  are the random, uncoupled functions, we arrive at the following expression:

$$\int_V (\nabla \cdot \mathbf{T}) \cdot \delta \mathbf{v} dV - \int_{S_p} (\mathbf{N} \cdot \mathbf{T} - \mathbf{p}^*) \cdot \delta \mathbf{v} dS - \int_V \delta \sigma (\nabla \cdot \mathbf{v}) dV = 0, \quad (6)$$

where  $\sigma = (1/3) I_1(\mathbf{T})$ , and  $\sigma \mathbf{g}$  the spherical part of the tensor  $\mathbf{T}$ . Setting the velocity  $\mathbf{v} = \mathbf{v}^*$  on the surface  $S_v$  implies that on this surface,  $\delta \mathbf{v} = 0$ , and the second integral can be calculated not only on the part  $S_p$ , but

on the entire surface  $S$  bounding the volume  $V$ . In this case, we can apply the Ostrograd–Haus theorem to the first term of the second integral given in (6):

$$\int_S \mathbf{N} \cdot \mathbf{T} \cdot \delta \mathbf{v} dS = \int_V \nabla \cdot (\mathbf{T} \cdot \delta \mathbf{v}) dV,$$

and using the easily checked relation  $\nabla \cdot (\mathbf{A} \cdot \mathbf{b}) = (\nabla \cdot \mathbf{A}) \cdot \mathbf{b} + \mathbf{A}^T \cdot (\nabla \mathbf{b})$ , where  $\mathbf{A}$  is any tensor of the second rank,  $\mathbf{b}$  is any vector, represent the integral in the right-hand part in the following form (under the assumption that  $\mathbf{A} = \mathbf{T}$ ,  $\mathbf{b} = \delta \mathbf{v}$  and with account of the symmetry of the tensor  $\mathbf{T}$ ):

$$\int_V \nabla \cdot (\mathbf{T} \cdot \delta \mathbf{v}) dV = \int_V (\nabla \cdot \mathbf{T}) \cdot \delta \mathbf{v} dV + \int_V \mathbf{T} \cdot \nabla (\delta \mathbf{v}) dV.$$

As a result, equation (6) can be rewritten as

$$\int_{S_p} \mathbf{p}^* \cdot \delta \mathbf{v} dS - \int_V \delta \sigma (\nabla \cdot \mathbf{v}) dV - \int_V \mathbf{T} \cdot \nabla (\delta \mathbf{v}) dV = 0. \quad (7)$$

Then, we transform the integrand in the last integral in (7) to:

$$\begin{aligned} \mathbf{T} \cdot \nabla (\delta \mathbf{v}) &= (\sigma \mathbf{g} + \mathbf{S}) \cdot \nabla (\delta \mathbf{v}) = \sigma \mathbf{g} \cdot \nabla (\delta \mathbf{v}) + \mathbf{S} \cdot \nabla (\delta \mathbf{v}) = \sigma \mathbf{R}^i \mathbf{R}_i \cdot \mathbf{R}^k \frac{\partial}{\partial q^k} (\delta \mathbf{v}) + \mathbf{S} \cdot \nabla (\delta \mathbf{v}) = \\ &= \sigma \mathbf{R}^i \cdot \frac{\partial}{\partial q^i} (\delta \mathbf{v}) + \mathbf{S} \cdot \nabla (\delta \mathbf{v}) = \sigma \nabla \cdot (\delta \mathbf{v}) + \mathbf{S} \cdot \nabla (\delta \mathbf{v}). \end{aligned} \quad (8)$$

Here, it is taken into account that  $\sigma \mathbf{g}$  is the spherical part of the tensor  $\mathbf{T}$ ,  $\mathbf{g} = \mathbf{R}^i \mathbf{R}_i$  is one of the representations of the unit tensor, where  $\mathbf{R}_i$ ,  $\mathbf{R}^i$  are the vectors of the main and mutual bases, respectively, and the Hamiltonian operator in the current state is written as  $\nabla = \mathbf{R}^k \partial / \partial q^k$ . According to the law of plastic flow  $\mathbf{S} = (2\bar{\sigma} / 3\dot{\bar{\epsilon}}) \dot{\bar{\epsilon}}$ , and so the last term of the final expression (8) takes the following form:

$$\mathbf{S} \cdot \nabla (\delta \mathbf{v}) = \mathbf{S} \cdot \delta (\nabla \mathbf{v}) = \mathbf{S} \cdot \frac{1}{2} [\delta (\nabla \mathbf{v}) + \delta (\nabla \mathbf{v})^T] = \mathbf{S} \cdot \dot{\bar{\epsilon}} = \frac{2\bar{\sigma}}{3\dot{\bar{\epsilon}}} \dot{\bar{\epsilon}} \cdot \delta \dot{\bar{\epsilon}} = \frac{2\bar{\sigma}}{3\dot{\bar{\epsilon}}} \frac{3\delta \dot{\bar{\epsilon}}^2}{2} = \bar{\sigma} \delta \dot{\bar{\epsilon}}. \quad (9)$$

The derivation of (9) is performed using the following postulates:

1) In this case and only in this case the Hamiltonian operator of the current state and the variation operator are interchangeable for one another (commutate). Indeed, the position of the point in the current state is determined by the radius-vector  $\mathbf{R} = \mathbf{r} + \mathbf{u}$ , where  $\mathbf{r}$  is the position of the point in the initial configuration,  $\mathbf{u}$  is the displacement vector. According to the Jourdain principle, the variation of the displacement velocity does not imply the variation of the displacement itself (remains invariable). Therefore, the quantity  $\mathbf{R}$ , as well as all quantities determined in terms of  $\mathbf{R}$ , such as the basis vectors  $\mathbf{R}_i$  and  $\mathbf{R}^i$ , also remain unvaried. Hence,  $\nabla (\delta \mathbf{v}) = \mathbf{R}^i \partial (\delta \mathbf{v}) / \partial q^i = \delta (\mathbf{R}^i \partial \mathbf{v} / \partial q^i) = \delta (\nabla \mathbf{v})$ . From the above it follows that this commutation would be impossible if variation of the displacement was performed (as in the Lagrangian principle), since the basis vector would also vary. In such a case it would be necessary to proceed to the Hamiltonian operator of the initial state, which is commutable with the variation operator.

2) The double scalar product of tensors of the second rank has the following property:  $\mathbf{A} \cdot \cdot \mathbf{B} = \mathbf{A}^T \cdot \cdot \mathbf{B}^T$ , and the tensor  $\mathbf{S}$  is symmetric. Therefore  $\mathbf{S} \cdot \cdot \delta (\nabla \mathbf{v}) = \mathbf{S} \cdot \cdot \delta (\nabla \mathbf{v})^T$ .

Substituting (9) into (8), and then the latter into (7) gives the final version of the variational equation:

$$\int_V \bar{\sigma} \delta \dot{\bar{\epsilon}} dV - \int_{S_p} \mathbf{p}^* \cdot \delta \mathbf{v} dS + \int_V [\sigma (\nabla \cdot \delta \mathbf{v}) + (\nabla \cdot \mathbf{v}) \delta \sigma] dV = 0. \quad (10)$$

In (10), the volume and surface again pertain to the current state and are unknown until the problem is solved. Using the same manipulation as in transition from equation (3) to equation (4), we can reduce (10) to the constructive form:

$$\int_{V_0} J \bar{\sigma} \delta \bar{\varepsilon} dV_0 - \int_{S_p} J \sqrt{\mathbf{n} \cdot \mathbf{C}^{-1} \cdot \mathbf{n}} \mathbf{p}^* \cdot \delta \mathbf{v} dS_{p_0} + \int_{V_0} J [\sigma (\nabla \cdot \delta \mathbf{v}) + (\nabla \cdot \mathbf{v}) \delta \sigma] dV_0 = 0. \quad (11)$$

The variational equation (11), describing the thermomechanical behavior of the medium, is supplemented with heat equation (5) for temperature variation, and these equations are interrelated. They are nonlinear, and their solution is based on the application of a stepwise loading procedure. The procedure makes it possible to trace the deformation history, which is important when using the law of plastic flow, and also to perform linearization of the resulting equations at each step.

The unsteady thermal conductivity equation (5) used in studying the upsetting process takes into account the internal source of heat release as a result of plastic deformation:  $Q = \gamma \bar{\sigma} \dot{\bar{\varepsilon}}$ , W/m<sup>3</sup>, where the coefficient of conversion of mechanical energy into thermal energy  $\gamma$  is taken equal to 0,9 [9]. Under plastic deformation, the coefficient of convective heat transfer between the billet and plates has a value of 11 kW/(m<sup>2</sup>·K) [9]. As the initial conditions we used the estimated temperature distribution in the body, which is formed at the first stage of modeling — during cooling of the billet in the air, as it is transported from the furnace to the deforming equipment. The ambient temperature in the process of hot forging is assumed to be 20°C.

Under the action of friction forces arising between the contact surfaces of the billet and the deforming plates, the billet at the final stage of the upsetting process takes the form of a single barrel with a convex lateral surface, as shown in Figure 5,*a*.

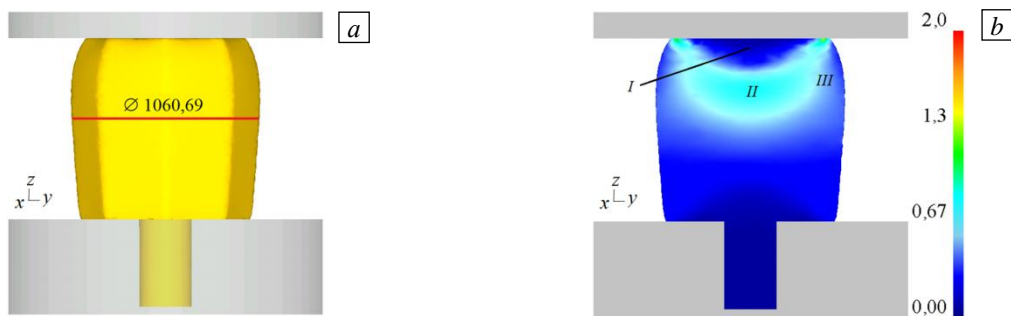


**Fig. 5.** Shape of the billet lateral surface (*a*) and distribution of plastic strain intensity (*b*) at the end of the upsetting process: zones *I*, *III* – constrained deformation and *II* – intensive deformation.

In the presence of frictional forces between the contacting surfaces of the billet and plates, the radial flow of the alloy is hindered, which leads to generation of constrained deformation areas in the billet under the plates. Thus, the process of free upsetting of the billet culminates in the formation of three zones (see Fig. 5,*b*), which are characterized by a significant difference in the intensity of accumulated plastic deformation. Zone *I* is adjacent to the contact surface of the upper plate and has a dome shape. In this zone, the value of accumulated plastic strain intensity averages 0,114. In zone *II*, the value of accumulated plastic strain intensity reaches the highest value of 0,798, while at the periphery, in zone *III*, it is equal to 0,48. Zone *I* is the zone of minimum values of accumulated plastic strain intensity. These data agree with the information from the literature sources [6, 7].

In order to illustrate the results of numerical calculations carried out for simulating the process of billet upsetting, we marked three points belonging to zones *I–III* on the vertical section passing through the central axis. The calculated values of temperature distribution and temperature variation with the movement of the upper plate at the selected points are shown in Figure 6. At point *I*, the value of temperature at the end of the upsetting operation is 1004,5°C, at point 2 — 1042,7°C, at point 3 — 1024,6 (see Fig. 6*b*). In the region of intense plastic deformation (in zone *II*), increase in temperature (metal heating) is  $\Delta T = 42,7$  °C; it occurs due to the work done by plastic deformation. The highest temperature value of 1070 °C is observed at the periphery of the billet in the zone of contact with the deforming equipment. For comparison, in work [1], the values of temperature at the same points obtained without considering air cooling of the billet are as follows: *I* — ~1006,03°C, 2 — ~1041,59°C, 3 — ~1024,64°C (curves 4–6, see Fig. 6*b*).

Thus, taking into account the initial inhomogeneous temperature distribution formed as a result of billet transporting from the furnace to the equipment, causes in general a growth of temperature during upsetting, although in the "narrow" near-surface zone (see zones I and III) it is slightly lower than in the variant when this cooling is disregarded. And vice versa, in the central part of the billet (zone II) the temperature is higher than in the process without pre-cooling. This is due to an increase in the work, which is converted into heat as a result of plastic deformation. The intensity of plastic deformation in zone II is higher if the technological process is modeled taking into account cooling of the billet in air during its transportation to the deforming equipment, compared to modeling of the process without this cooling. This accounts for an increase in work as compared to the process disregarding cooling.

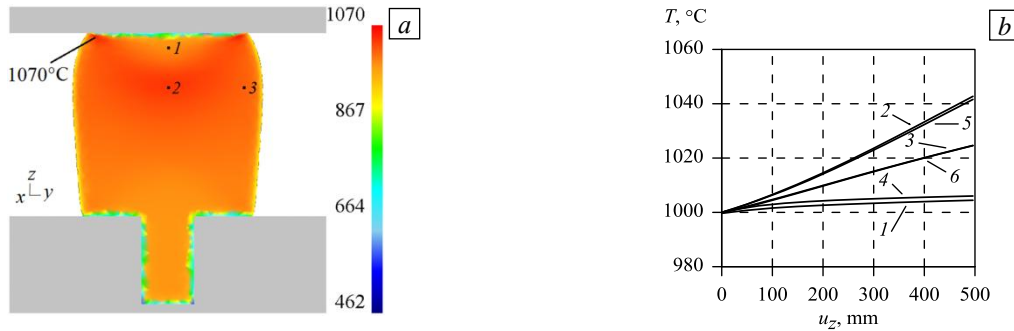


**Fig. 6.** Temperature distribution in the vertical axial section of the billet (a) and its dependence on the displacement of the upper plate at the three selected points (b): taking into account (curves 4–6) and disregarding (1–3) cooling of the billet as it is transported from the furnace to the upsetting equipment.

On the upper surface of the billet, the average temperature at the end of the upsetting process is  $\sim 614^\circ\text{C}$ , and on its lower surface it is  $\sim 690^\circ\text{C}$ . On the shank surface, the temperature varies from  $690^\circ\text{C}$  to  $614^\circ\text{C}$ , and on its lower end surface is  $\sim 538^\circ\text{C}$ . On the sharp ribs of the billet, the temperature reaches a value of  $\sim 886^\circ\text{C}$ , but these areas cool down faster than the rest of the billet. Figure 6a shows that the temperature decrease extends into the central region of the billet by not more than  $\sim 30$  mm.

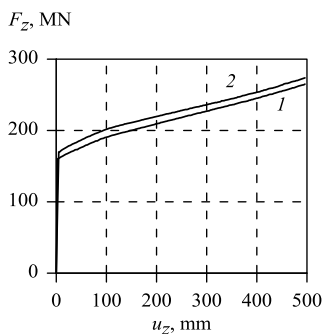


**Fig. 7.** Dependence of the deformation force on the displacement of the upper plate moving with a speed of 100 mm/s disregarding (curve 1) and taking into account (2) the billet cooling during transportation.

The process of free upsetting requires a large amount of energy and power. The deformation mode is selected depending on the force and power required to perform a specific technological operation. According to the performed numerical simulation, the required force is 273 MN, which is about 3% higher than the force calculated without taking into account the air cooling of a solid billet during its transportation (see [1]). Due to a decrease in temperature by the time of forging, the press should provide a higher force.

The variation of force required for the average axial deformation during upsetting by the amount of  $\sim 32,5\%$ , as a function of the movement of the upper plate is plotted in Figure 7. The curve has a monotonically increasing character. As is seen from the plot, the calculated value of force required to implement the upsetting process of a large billet to average axial deformation of 32,5% is rather high. In pressure forming of large-size workpieces (with mass over 350 kg), such force (from 50 MN to 750 MN) can be developed, for example, by powerful hydraulic presses (including modern isostatic presses for hot pressing to 400 MN), whereas the power of modern forging press is only 185 MN [15, 16]. However, it is possible to reduce the load to a value, at which the technological process under consideration can be realized on a hydraulic press of less power. To this end, the billet is heated in the furnace to a higher forging temperature of  $1150\text{--}1200^\circ\text{C}$  [17]. In addition, it should be taken into account that the surface of the billet cools down rather quickly, by about  $50^\circ\text{C}$  for 45 seconds at ambient temperature of  $20^\circ\text{C}$ . Therefore, the transfer of the billet from the furnace to the forging equipment should be as fast as possible.

#### 4. Results of simulation of microstructure changes in the Waspaloy nickel alloy during dynamic recrystallization

At present, there are many mathematical models and a variety of their modifications that allow predicting changes in the structure of polycrystalline bodies in the process of recrystallization. These models are based on either the Monte Carlo method [18], or the phase field method [19], or cellular automata [20, 21]. In [22, 23], the description of microstructure of polycrystals is based on the models using dislocation density.

In this study, the structure formation in a nickel alloy during its upsetting is investigated by the Johnson-Mel-Avrami-Kolmogorov (JMAK) phenomenological model [24-27], with its modification being implemented in the Deform-2D/3D software package. The analysis of publications concerned with the models, which are based on the Kolmogorov and Avrami equations shows good agreement between the results of numerical and physical experiments. The JMAK model is based on the supposition that nuclei of new grains appear in a material randomly and then grow to replace other grains. The relations of the JMAK model allow us to calculate the average grain size and the fraction of recrystallized volume as a function of strain and temperature. The JMAK model has been used for many years in the aerospace industry to predict grain size in high temperature alloys. Therefore, this model is used here as the most effective tool for describing the microstructure evolution.

The process of dynamic recrystallization occurs during deformation, when the strain intensity exceeds the critical value  $\bar{\varepsilon}_c$ , which is defined by the following relation:

$$\bar{\varepsilon}_c = a_0 \bar{\varepsilon}_p. \quad (12)$$

Here:  $\bar{\varepsilon}_p = a_1 d_0^{n_1} \dot{\varepsilon}^{m_1} \exp(Q_1/RT) + c_1$  is the peak strain intensity, at which the stress intensity reaches the maximum value in the uniaxial strain diagram « $\sigma - \varepsilon$ »;  $d_0$  is the initial grain size,  $\mu\text{m}$ ;  $\dot{\varepsilon}$  is the effective strain rate,  $\text{s}^{-1}$ ;  $T$  is material temperature on the absolute scale, K;  $R = 8,31 \text{ J}/(\text{mol} \cdot \text{K})$  is the universal gas constant.

The size of dynamically recrystallized grains  $d_{drex}$  and their volume fraction  $X_{drex}$  are determined by the expressions [8, 28–30]:

$$d_{drex} = a_3 d_0^{h_3} \bar{\varepsilon}^{n_3} \exp(Q_3/RT) + c_3 \quad (\text{если } d_{drex} \geq d_0, \text{ тогда } d_{drex} = d_0), \quad (13)$$

$$X_{drex} = 1 - \exp \left[ -\beta_d \left( \frac{\bar{\varepsilon} - \bar{\varepsilon}_c}{\bar{\varepsilon}_{0,5}} \right)^{k_d} \right], \quad \bar{\varepsilon} \geq \bar{\varepsilon}_c, \quad (14)$$

where  $\bar{\varepsilon}$  is the effective strain,  $\beta_d$  is the temperature-dependent growth factor and  $k_d$  is the exponential coefficient of nuclei formation. The average size of dynamically recrystallized grains is determined by the initial material microstructure ( $d_0$ ) and the deformation mode ( $\bar{\varepsilon}$ ). The strain rate at the 50% recrystallization is calculated by the formula:

$$\bar{\varepsilon}_{0,5} = a_2 d_0^{h_2} \bar{\varepsilon}^{n_2} \dot{\varepsilon}^{m_2} \exp(Q_2/RT) + c_2. \quad (15)$$

The final average grain size  $d_{averg}$  is determined from the relation:

$$d_{averg} = X_{drex} d_{drex} + (1 - X_{drex}) d_0. \quad (16)$$

In relations (12) – (15),  $Q_{1\pm 3}$  are the activation energies,  $\text{kJ}/\text{mol}$ ;  $a_{0\pm 3}$ ,  $n_{1\pm 3}$ ,  $m_{1\pm 3}$ ,  $c_{1\pm 3}$ ,  $h_{1\pm 3}$  are the coefficients, characterizing the material properties under specified deformation conditions. The values of these coefficients are determined based on the metallographic studies and physical experiments, in which the cylindrical specimens are subject to compressive loads under different deformation conditions, as described in detail in [1]. For some materials they are given in the scientific literature. For the Waspaloy nickel alloy, the coefficients in the JMAK expressions (12) – (15) were borrowed from the standard database of the DEFORM–2D/3D software package and presented in paper [1]. The initial grain size was taken to be 25  $\mu\text{m}$ .

### 5. Results of computer simulation of dynamic recrystallization process in Waspaloy alloy during hot deformation

The upsetting of a Waspaloy alloy specimen with a cooled near-surface region by an upper plate moving with a speed of 100 mm/s leads to the formation of inhomogeneous strain and temperature distributions in the specimen. This, in turn, causes the formation of an inhomogeneous material structure (see Fig. 8a): there are zones with partial recrystallization (II, III) and a zone, where recrystallization is negligible (I). The calculated values of the volume fraction of the material experiencing dynamic recrystallization after completion of the free upsetting process are ~0,0006 at point I, which belongs to zone I, ~0,769 at point 2, which is in the region of intense plastic deformation, and ~0,365 at point 3 in zone III (see Fig. 8a). The average value of the volume fraction of the dynamically recrystallized portion of the material is approximately 0,327, i.e., only a small portion of the material is involved in this process.

Figure 8b shows the variation in the size of dynamically recrystallized grains depending on the displacement of the upper plate  $u_z$  at three selected points. Thus, at the end of the process of free upsetting the calculated values of  $d_{drex}$  determined by formula (13), are as follows: 2,24  $\mu\text{m}$  in the vicinity of point I, 10,3  $\mu\text{m}$  in the vicinity of point 2, and 10,6  $\mu\text{m}$  in the vicinity of point 3. As is evident from Fig. 8, in the zone of intense plastic deformation the dynamically recrystallized grains have a smaller size as compared to the size of grains in zone III. The reason is that in zone II the density of recrystallization nuclei formed during hot deformation is higher, which impedes their further growth. During upsetting, zone I is the closest to the upper plate and is characterized by constrained deformation. Therefore, the smallest dynamically recrystallized grains are found in the vicinity of point I. The value of temperature at point I calculated without taking into account the transport of the billet by air is higher than the value calculated with account of the cooling process and is ~1010°C. Therefore, the curve  $d_{drex}$  in the vicinity of this point is located higher (see Fig. 8b, curve 4). In zones II and III, the sizes of dynamically recrystallized grains near points 2 and 3 at the end of the upsetting process are practically similar.

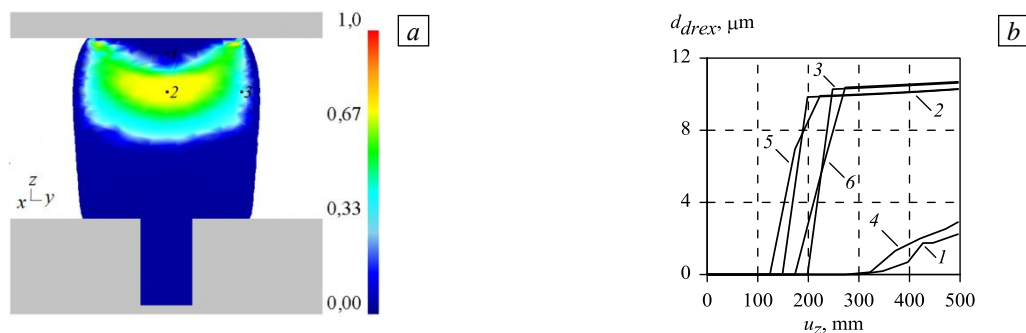


**Fig. 8.** The fraction of grains in the axial section of the billet experienced dynamic recrystallization at the end of the upsetting process that (a) and changes in the size of these grains depending on  $u_z$  taking into account ( $I^o-3^o$ ) and disregarding (1–3) the billet cooling in air (b).

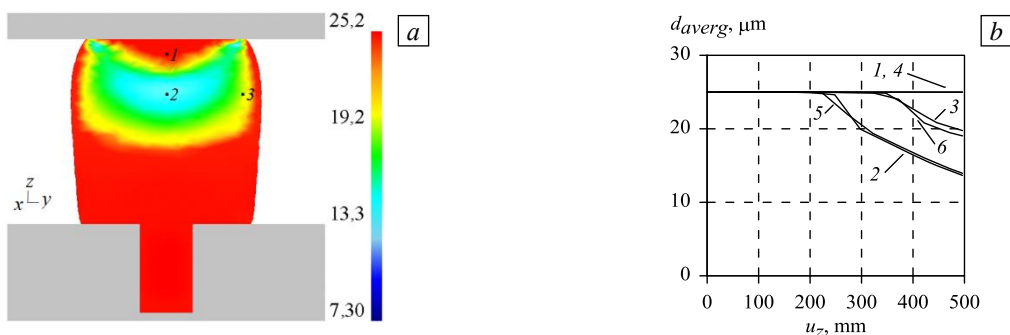


**Fig. 9.** Distribution of the average grain size  $d_{averg}$   $\mu\text{m}$  in the vertical section of the ingot (a) and its dependence on the movement of the upper striker at characteristic points, taking into account (curves 1–3) and without taking into account (4–6) cooling of the billet in air.

Figure 9 shows the distribution of the average grain size and the curves of changes in the final average size as a function of  $u_z$  at the three selected points obtained with and without consideration for cooling of the billet during its transportation by air. It can be seen that in the vicinity of point *I*, the average grain size does not change after the completion of the deformation process and is 25  $\mu\text{m}$ . In the vicinity of point 2, the average grain size is almost 2 times smaller as compared to the initial state: 13,7  $\mu\text{m}$  compared to the initial size of 25  $\mu\text{m}$ . This is about 0,2  $\mu\text{m}$  smaller than in the case of disregarding the air cooling of the billet during its transportation from the furnace to the press. In the vicinity of point 3, the average grain size changes insignificantly and is 19,8  $\mu\text{m}$ , which is greater by about 0,8  $\mu\text{m}$  than in the case when cooling of the billet is not taken into account. The grains subjected to the most intensive deformation (see Fig. 9b) experience the greatest refinement (see Fig. 5b). This occurs in the central zone *II* of the billet, where the process of dynamic recrystallization proceeds more intensively compared to the process at the periphery (in zone *III*). Moreover, pre-cooling of the billet during its air transportation intensifies this process. At the same time, about 67,3% of all grains retain their average size after deformation, which is by ~9,39% more than in the case when cooling of a massive billet in air during its transportation from the furnace to the deforming press is not taken into account.

## 6. Conclusion

In this study, we have performed the temperature analysis of the process of transporting the billet of heat resistant Waspalloy nickel alloy from the furnace to the deforming equipment and complete deformation and the temperature analysis of the billet upsetting. The obtained results have confirmed the possibility of using Johnson–Mei–Avrami–Kolmogorov model implemented in the Deform–2D/3D software package for the description of microstructure changes in the examined alloy during dynamic recrystallization. At a displacement speed of the upper die of 100 mm/s, the average grain size in the zone of intensive plastic deformation (in zone *II*) decreases almost twice compared to the initial size of 25  $\mu\text{m}$  and is 13,7  $\mu\text{m}$ . In the peripheral regions (zones *I* and *III*), where deformation is practically absent or small, grain crushing is insignificant. The average value of the volume fraction of dynamically recrystallized material is approximately 0,327.

Consideration of billet cooling in air during its transportation within 45 s from the furnace to the deforming equipment leads to a change in the temperature field in the narrow near-surface region by about 47°C. As a consequence, the force that should be developed by the press increases by ~3%, and the fraction of the uncrystallized part of the material increases by 9,39% compared to the process, where cooling is not considered. A decrease in temperature at forging time leads to an increase in the average grain size in the zones of constrained deformation (in zone *I* — insignificantly, in zone *II* — by ~0,8  $\mu\text{m}$ ), and to a decrease by ~0,2  $\mu\text{m}$  in the central part of the billet.

## References

1. Rogovoy A.A., Salikhova N.K. Numerical investigation of the evolution of microstructure of nickel-based alloys during plastic working. *Vychis. mekh. splosh. sred – Computational continuum mechanics*, 2019, vol. 12, no. 3, pp. 271-280. <https://doi.org/10.7242/1999-6691/2019.12.3.23>
2. Gorelik S.S., Dobatkin S.V., Kaputkina L.M. *Rekristallizatsiya metallov i splavov* [Recrystallization of metals and alloys]. Moscow, MISIS, 2005. 432 p.
3. Hässner F. (ed.) *Recrystallization of metallic materials*. Dr. Riederer Verlag, 1978. 293 p.
4. Bernshteyn M.L. *Struktura deformirovannykh metallov* [The structure of deformed metals]. Moscow, Metallurgiya, 1977. 432 p.
5. Gromov N.P. *Teoriya obrabotki metallov davleniyem* [Theory of metal forming.]. Moscow, Metallurgiya, 1978. 360 p.
6. Okhrimenko Ya.M., Tyurin V.A. *Teoriya protsessov kovki* [Theory of forging processes]. Moscow, Vysshaya shkola, 1977. 295 p.
7. Semenov E.I. (ed.) *Kovka i shtampovka: Spravochnik. T. 1. Materialy i nagrev. Oborudovaniye. Kovka* [Forging and Stamping: A handbook. Vol. 1. Materials and heating. Equipment. Forging]. Moscow, Mashinostroyeniye, 1985. 568 p.
8. *DEFORM<sup>TM</sup> 3D Version 6.1 (sp2). User's Manual*. Scientific Forming Technologies Corporation, 2008. 415 p.
9. *Prakticheskoye rukovodstvo k programnomu kompleksu DEFORM-3D* [A practical guide to the DEFORM-3D software package]. Ekaterinburg: UrFU, 2010. 266 p.

10. Samarskiy A.A., Vabishchevich P.N. *Vychislitel'naya teploperedacha* [Computational heat transfer]. Moscow, Editorial URSS, 2003. 784 p.
11. Kobayashi S., Oh S., Altan T. *Metal forming and the finite element method*. Oxford University Press, 1989. 377 p.
12. Ivanov K.M. (ed.) *Prikladnaya teoriya plastichnosti* [Applied theory of plasticity]. St. Petersburg, Politekhnik, 2011. 375 p.
13. Unksov E.P., Ovchinnikov A.G. (ed.) *Teoriya plasticheskikh deformatsiy metallov* [Theory of plastic deformations of metals]. Moscow, Mashinostroyeniye, 1983. 598 p.
14. Isachenko V.P., Osipov V.A., Sukomel A.S. *Teploperedacha* [Heat transfer]. Moscow, Energoizdat, 1981. 416 p.
15. Zhavoronkov N.M. (ed.) *Legkiye i zharoprochnyye splavy i ikh obrabotka* [Light and heat-resistant alloys and their processing]. Moscow, Nauka, 1986. 304 p.
16. <https://www.wepuko.de/ru/gidravlicheskie-kovochnye-pressy/produkcija/pressy-svobodnoi-kovki/> (accessed 1 June 2021).
17. Storozhev M.V. (ed.) *Kovka i ob'yemnaya shtampovka stali. Spravochnik. T. 2.* [Forging and die forging of steel. A handbook. Vol. 2]. Moscow, Mashinostroyeniye, 1968. 448 p.
18. Srolovitz D.J., Grest G.S., Anderson M.P. Computer simulation of grain growth – V. Abnormal grain growth. *Acta metall.*, 1985, vol. 33, pp. 2233-2247. [https://doi.org/10.1016/0001-6160\(85\)90185-3](https://doi.org/10.1016/0001-6160(85)90185-3)
19. Meccozzi V.G., Eiken J., Santofimia M.J., Sietsma J. Phase field modeling of microstructural evolution during the quenching and partitioning treatment in low-alloy steels. *Comput. Mater. Sci.*, 2016, vol. 112, part A, pp. 245-256. <https://doi.org/10.1016/j.commatsci.2015.10.048>
20. An D., Pan S., Huang L., Dai T., Krakauer B., Zhu M. Modeling of ferrite-austenite phase transformation using a cellular automation model. *ISIJ Int.*, 2014, vol. 54, pp. 422-429. <https://doi.org/10.2355/isijinternational.54.422>
21. Raabe D. Cellular automata in materials science with particular reference to recrystallization simulation. *Annu. Rev. Mater. Res.*, 2002, vol. 32, pp. 53-76. <https://doi.org/10.1146/annurev.matsci.32.090601.152855>
22. Bergstrom Y. A dislocation model for the stress-strain behaviour of polycrystalline  $\alpha$ -Fe with special emphasis on the variation of the densities of mobile and immobile dislocations. *Mater. Sci. Eng.*, 1970, vol. 5, pp. 193-200. [https://doi.org/10.1016/0025-5416\(70\)90081-9](https://doi.org/10.1016/0025-5416(70)90081-9)
23. Lopatin N.V., Gorbushina S.N., Dyakonov G.S., Kydriavchev E.A., Vidumkina S.V. Simulation of microstructure evolutions of vt6 alloy during isothermal forging using Deform software. *Komp'yuternyye issledovaniya i modelirovaniye – Computer Research and Modeling*, 2014, vol. 6, no. 6, pp. 975-982. <https://doi.org/10.20537/2076-7633-2014-6-6-975-982>
24. Avrami M. Kinetics of phase change. I. General theory. *J. Chem. Phys.*, 1939, vol. 7, pp. 1103-1112. <https://doi.org/10.1063/1.1750380>
25. Avrami M. Kinetics of phase change. II. Transformation-time relations for random distribution of nuclei. *J. Chem. Phys.*, 1940, vol. 8, pp. 212-224. <https://doi.org/10.1063/1.1750631>
26. Avrami M. Kinetics of phase change. III. Granulation, phase change, and microstructure. *J. Chem. Phys.*, 1941, vol. 9, pp. 177-184. <https://doi.org/10.1063/1.1750872>
27. Johnson W.A., Mehl R.F. Reaction kinetics in process of nucleation and growth. *Trans. Am. Inst. Min. Met. Eng.*, 1939, vol. 135, pp. 416-442.
28. Alimov A.I., Voronezhskiy E.V. *Matematicheskoye modelirovaniye evolyutsii mikrostruktury pokovki v protsesse termomekhanicheskoy obrabotki* [Mathematical modeling of the evolution of the forging microstructure during thermomechanical processing]. *Nauka i obrazovaniye – Science and Education*, 2011, no. 8, 15 p.
29. Sellars C.M., McTegart W.J. On the mechanism of hot deformation. *Acta Metall.*, 1966, vol. 14, pp. 1136-1138. [https://doi.org/10.1016/0001-6160\(66\)90207-0](https://doi.org/10.1016/0001-6160(66)90207-0)
30. Sellars C.M. The kinetics of softening process during hot working of austenite. *Czech. J. Phys.*, 1985, vol. 35, pp. 239-248. <https://doi.org/10.1007/BF01605090>

The authors declare no conflict of interests.

The paper was received on 24.04.2021.

The paper was accepted for publication on 14.05.2021.